Computer Assisted Methods in Engineering and Science, **26**: 5–19, 2019, doi: 10.24423/cames.252

IPM 2019

Estimation of the ischemic brain temperature with the particle filter method

Felipe S. Nunes[1], Helcio R.B. Orlande[1], Andrzej J. Nowak[2]
[1] *Department of Mechanical Engineering, Politecnica/COPPE*
Federal University of Rio de Janeiro
Cid. Universitaria, Cx. Postal: 68503, Rio de Janeiro, RJ, 21941-972, Brazil
e-mail: fsantannan@gmail.com, helcio@mecanica.coppe.ufrj.br
[2] *Institute of Thermal Technology, Silesian University of Technology*
Konarskiego 22, 44-100 Gliwice, Poland
e-mail: Andrzej.J.Nowak@polsl.pl

In this work, a two-dimensional model was developed to analyze the transient temperature distribution in the head of a newborn human, during local cooling promoted by the flow of cold water through a cap. The inverse problem dealt with the sequential estimation of the internal temperature of the head, by performing non-invasive transient temperature measurements. A state estimation problem was solved with the sampling importance resampling (SIR) algorithm of the particle filter method. Uncertainties in the evolution and observation models were assumed as additive, Gaussian, uncorrelated and with zero means. The uncertainties for the evolution model were obtained from the Monte Carlo simulations, based on the uncertainties of the model parameters. The head temperature was accurately predicted with the particle filter method. Such a technique might be applied in the future to monitor the brain temperature of newborns and control the local cooling treatment of neonatal hypoxic-ischemic encephalopathy.

Keywords: neonatal hypoxic-ischemic encephalopathy, particle filter method, sampling importance resampling (SIR) algorithm, local cooling technique.

Nomenclature

c	–	specific heat,
h	–	global heat transfer coefficient,
H	–	thickness of the channel,
k	–	thermal conductivity,
$\dot{m}$	–	cooling water mass flow rate,
N	–	number of particles,
q	–	metabolic volumetric heat generation rate,
r	–	radial spatial variable,
T	–	temperature,
T_a	–	arterial blood temperature,
T_0	–	initial temperature distribution in the head,
T_∞	–	initial water temperature and surrounding temperature,
w	–	particle weight,
$\mathbf{y}$	–	vector of state variables,
$\mathbf{z}$	–	vector with the prediction of the measurements.

Greek symbols:

$\boldsymbol{\theta}$ – vector of non-dynamic model parameters,
θ – angular spatial variable,
ρ – density,
τ – time,
ω – perfusion coefficient.

Subscripts:

b – blood,
gm – gray matter,
k – time instant,
l – cooling water,
sc – scalp,
sk – skull,
t – tissue,
wm – white matter.

Superscripts:

i – particle index,
$meas$ – measurements.

1. Introduction

This study is focused on the neonatal hypoxic-ischemic encephalopathy (HIE), which is a neurological disorder observed in newborn babies, commonly caused by birth asphyxia [1]. An inadequate oxygen supply to the brain, due to low blood flow, immediately causes necrotic cell death, which is then followed by the second phase of HIE that is characterized by cerebral edema and cell apoptosis. This second phase takes place between 6 and 72 hours after the blood supply to the brain is decreased [1]. An efficient treatment to reduce brain damage and death of the newborn is to decrease the body core temperature to around 34°C for a period of at least 72 hours. Cooling should be started within the first phase of HIE, in order to increase the chances of successful treatment [1–8].

Both systemic and local cooling techniques have been used for the treatment of the neonatal hypoxic-ischemic encephalopathy, and commercial products are currently available for medical practice [1–10]. Systemic cooling can be achieved by surrounding the body of the newborn, except the head, with a cooling blanket containing channels through which cold water is circulated around a body. The rate of temperature reduction is slower with the systemic cooling than with the local cooling. Additionally, the systemic technique also produces the cooling of other vital regions, and undesirable physiological side-effects are more likely to occur, such as cardiac arrhythmia, venous thrombosis and hypotension [1, 6]. On the other hand, the systemic cooling technique offers the advantage such that the head of the newborn can be easily accessed for examinations or other medical interventions. Local cooling can be achieved with the flow of cold water through a cap surrounding the newborn's head, while the remaining body can be warmed by a radiator in the incubator. Therefore, the local technique provides neuroprotection with minimum side-effects due to hypothermia, by cooling the brain while maintaining the patient's core temperature at safe levels. The local technique is expected to be less aggressive to the body, however the access to the head is only allowed if the cooling cap is removed, which can significantly affect the treatment. Besides that, it has been shown that local cooling might not effectively reduce the brain temperature because of the blood perfusion that heats the head [11].

The temperature controlled during the cooling treatment is usually that of the core body, measured through the rectum [1–10]. Different techniques have been under development for the non-intrusive temperature measurement of internal tissues, for example, magnetic resonance [12] or photoacoustic technique [13, 14]. However, these techniques are currently in an experimental phase. Hence, the real-time measurement of the internal temperature of the brain is still not feasible. Computational simulation of bioheat transfer during the cooling process can provide estimates of the brain temperature. However, the numerical simulations involve uncertainties related to the conditions of the environment surrounding the newborn, as well as uncertainties related to the physical properties and shapes of organs, which vary from individual to individual, and even vary for the same individual, depending on the physiological conditions.

In state estimation problems, the information provided by measurements and numerical simulations, with their inherent uncertainties, is jointly used to produce sequential estimates of the desired dynamic variables. Particle filter methods provide a powerful and robust technique for the solution of state estimation problems, with results more accurate than those obtained with the available extensions of the Kalman filter, for nonlinear and non-Gaussian models [15–25].

In this work, the sampling importance resampling (SIR) algorithm of the particle filter is applied for the estimation of the transient internal temperature of the head during the local cooling treatment of the neonatal hypoxic-ischemic encephalopathy. Such an inverse problem is solved with numerically simulated temperature measurements of the water at the outlet of the cooling cap, as well as measurements taken at specific points on the head surface.

The considered physical problem and its mathematical formulation are presented in the next section, which is followed by the definition of the state estimation problem and the presentation of the sampling importance resampling (SIR) algorithm of the particle filter. Numerical results are then presented and discussed, including the selection of the number of particles for the SIR algorithm and the number of measurement locations, which are required for an accurate solution of the state estimation problem. The cases examined in this paper include a healthy brain, a brain with a partial ischemic region and a brain where ischemia takes place in the whole gray and white matters.

2. Physical problem and mathematical formulation

The physical problem considered here involves bioheat transfer in a multilayer hemisphere [9, 26]. The problem is considered to be axisymmetric, with perfect contact between the layers that correspond to white matter, gray matter, skull and scalp, as illustrated in Fig. 1. This figure also presents the water channel in the cooling cap. Physical properties of each layer are assumed to be constant. Heat transfer from the head to the cold water flowing through the cap is accounted for by a global heat transfer coefficient, which is assumed uniform over the surface. Heat transfer is neglected at the bottom surface of the hemisphere. Bioheat transfer is considered to follow Pennes' model [27] so that we can write for each tissue layer and for time $\tau > 0$:

$$\rho_t c_t \frac{\partial T_t(r,\theta,\tau)}{\partial \tau} = \frac{k_t}{r^2}\left[\frac{\partial}{\partial r}\left(r^2\frac{\partial T_t}{\partial r}\right) + \frac{1}{\sin\theta}\frac{\partial}{\partial \theta}\left(\sin\theta\frac{\partial T_t}{\partial \theta}\right)\right] + \rho_b c_b \omega_t(T_t)\left[T_a - T_t(r,\theta,\tau)\right] + q_t(T_t), \qquad (1)_1$$

where the subscript t designates the tissue layers, that is, $t = wm$ for white matter, $t = gm$ for gray matter, $t = sk$ for the skull and $t = sc$ for the scalp. The subscript b denotes blood, while ρ is the density, c is the specific heat, k is the thermal conductivity, ω is the perfusion coefficient, and T_a is the arterial blood temperature. The metabolic volumetric heat generation rate is denoted by q.

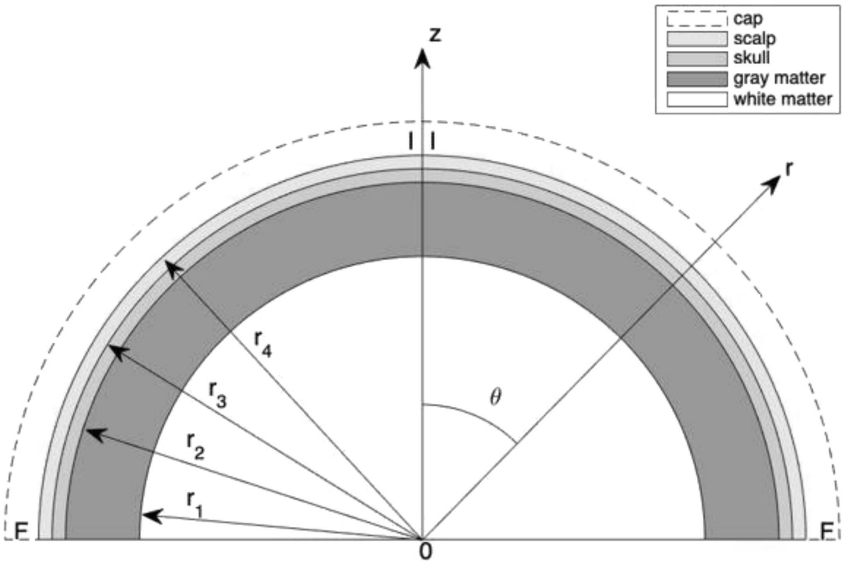

Fig. 1. The axisymmetric hemispherical region with multiple layers representing the head and the cooling cap.

The initial and boundary conditions for the problem are given respectively by:

$$T_t = T_0(r,\theta) \qquad \text{at} \quad \tau = 0, \qquad \text{in} \quad 0 < \theta < \frac{\pi}{2}, \quad 0 \le r < r_4, \tag{1}_2$$

$$\frac{\partial T_t}{\partial \theta} = 0 \qquad \text{at} \quad \theta = 0 \qquad \text{and} \quad \theta = \frac{\pi}{2}, \quad 0 \le r < r_4, \quad \tau > 0, \tag{1}_3$$

$$k_{sc}\frac{\partial T_{sc}}{\partial r} + hT_{sc} = hT_l(\theta,\tau) \qquad \text{at} \quad r = r_4, \quad 0 < \theta < \frac{\pi}{2}, \quad \tau > 0, \tag{1}_4$$

where $T_0(r,\theta)$ is the temperature distribution in the head at time $\tau = 0$, $T_l(\theta,\tau)$ is the temperature of the cooling water, and h is the global heat transfer coefficient between the head surface and the cooling water, which also accounts for all thermal resistances in the heat flow path.

With the perfect contact assumed between the layers, we can write:

$$k_{gm}\frac{\partial T_{gm}}{\partial r} = k_{wm}\frac{\partial T_{wm}}{\partial r} \qquad \text{and} \qquad T_{gm} = T_{wm} \quad \text{at} \quad r = r_1, \quad 0 < \theta < \frac{\pi}{2}, \quad \tau > 0, \tag{1}_5$$

$$k_{sk}\frac{\partial T_{sk}}{\partial r} = k_{gm}\frac{\partial T_{gm}}{\partial r} \qquad \text{and} \qquad T_{sk} = T_{gm} \quad \text{at} \quad r = r_2, \quad 0 < \theta < \frac{\pi}{2}, \quad \tau > 0, \tag{1}_6$$

$$k_{sc}\frac{\partial T_{sc}}{\partial r} = k_{sk}\frac{\partial T_{sk}}{\partial r} \qquad \text{and} \qquad T_{sc} = T_{sk} \quad \text{at} \quad r = r_3, \quad 0 < \theta < \frac{\pi}{2}, \quad \tau > 0. \tag{1}_7$$

The initial temperature distribution in the head $T_0(r,\theta)$, is given by the steady- state solution of the bioheat transfer (Eqs (1)), by assuming convection and linearized radiation heat transfer between the surface of the head and the surrounding environment before the water cooling takes place.

During the local cooling treatment of the neonatal hypoxic-ischemic encephalopathy that is considered here, water is assumed to flow through the channel inside the cooling cap from $\theta = 0$ to $\theta = \frac{\pi}{2}$, with a constant mass flow rate $\dot{m}$. The thickness of the channel H is small so that the temperature gradient in the radial direction is neglected. By neglecting heat transfer from the

surface of the cap to the surrounding environment the energy balance for the water in the cap is given by:

$$\frac{\partial T_l(\theta,\tau)}{\partial \tau} + \frac{\dot{m}}{2\pi r_4^2 H \rho_l \sin\theta}\frac{\partial T_l}{\partial \theta} = \frac{h}{H\rho_l c_l}\left[T_{sc}(r_4,\theta,\tau) - T_l(\theta,\tau)\right]$$

$$\text{in} \quad 0 < \theta < \frac{\pi}{2}, \qquad \text{for} \quad \tau > 0, \qquad (2)_1$$

where the subscript l denotes cooling water. The water enters the channel at the constant temperature $T_{l,I}$, and a local parabolic outflow boundary condition is assumed. The initial water temperature is T_∞. Thus,

$$T_l = T_{l,I} \qquad \text{at} \quad \theta = 0, \quad \tau > 0, \qquad (2)_2$$

$$\frac{\partial T_l}{\partial \theta} = 0 \qquad \text{at} \quad \theta = \frac{\pi}{2}, \quad \tau > 0, \qquad (2)_3$$

$$T_l = T_\infty \qquad \text{at} \quad \tau = 0, \qquad \text{in} \quad 0 < \theta < \frac{\pi}{2}. \qquad (2)_4$$

The perfusion coefficient and the metabolic heat generation rate are assumed to vary with temperature respectively in the form [1, 28]:

$$\omega_t(T_t) = \omega_{0t} 3^{\frac{[T_t(r,\theta,\tau)-T_a]}{10}} \qquad \text{and} \qquad q_t(T_t) = q_{0t} 3^{\frac{[T_t(r,\theta,\tau)-T_a]}{10}}. \qquad (3)$$

By following [9], the tissue baseline perfusion coefficient ω_{0t} is reduced to 20% of its original value during ischemia. The solution of the direct problem, where all model parameters, initial and boundary conditions are known, was obtained in this work with a dedicated finite volume code, which was verified with the COMSOL commercial finite element code.

3. State estimation problem and particle filter method

The objective of this work is to estimate the transient temperature at each finite volume used for the discretization of Eqs (1) to (3), by using non-invasive measurements of temperature at the surface of the head and the outlet of the cooling channel. Such an inverse problem is considered here in the form of a state estimation problem. The available measured data is then used together with the mathematical models for the physical phenomena and the measuring devices, in order to sequentially estimate the state variables [15–25].

The formulation of state estimation problems requires two stochastic mathematical models: the *evolution model*, which represents the discrete time evolution of the state variables, and the *observation model*, which provides a relationship between the measurements and the state variables [15–25]. The evolution and observation models can be respectively written in the following general forms [15–25]:

$$\begin{aligned} \mathbf{y}_k &= \mathbf{f}_k\left(\mathbf{y}_{k-1}, \boldsymbol{\theta}, \mathbf{v}_k\right), \qquad k = 1, ..., M, \\ \mathbf{z}_k &= \mathbf{g}_k\left(\mathbf{y}_k, \boldsymbol{\theta}, \mathbf{n}_k\right), \qquad k = 1, ..., M, \end{aligned} \qquad (4)$$

where $\mathbf{y}_k$ is the vector of state variables that describe the system at a given time instant t_k, $\mathbf{z}_k$ is the prediction of the measurements ($\mathbf{z}_k^{\text{meas}}$) and $\boldsymbol{\theta}$ is a vector containing all the non-dynamic parameters of the model. The vectors $\mathbf{v}_k$ and $\mathbf{n}_k$ represent the noises in the evolution and observation models, respectively. The probability density $\pi\left(\mathbf{y}_0, \boldsymbol{\theta} | \mathbf{z}_0\right) = \pi\left(\mathbf{y}_0, \boldsymbol{\theta}\right)$ at the initial time $t = 0$ is assumed as known for the solution of the state estimation problem [15–25].

In this work, the evolution model is given by the discrete forms of Eqs (1) to (3), and the state variables are the temperatures at all finite volumes used in the discretization. Since the measurements give the temperatures at specific locations, the observation model is simply a mapping of the evolution model, which selects the state variables at the measurement points.

The state estimation problem of this work is solved with the particle filter method [15–25]. In such a sequential Monte Carlo technique, the posterior probability density function of the state variables is represented by a set of random samples (particles) with associated weights. The particle filter method can be applied to nonlinear and non-Gaussian models since it is not restricted by the hypotheses required for the optimality conditions of the Kalman filter [15–25].

Each of the N particles representing the posterior distribution of the state variables at time t_k is denoted by $\mathbf{y}_k^i$, with corresponding weight w_k^i, where $i = 1, ..., N$. From the probability density at the initial time, $\pi(\mathbf{y}_0, \boldsymbol{\theta})$, a prior information for the state variables at the subsequent time t_1, is estimated by using the state evolution model, given by Eq. $(4)_1$. The observation model, given by Eq. $(4)_2$ and the actual measurements $\mathbf{z}_k^{\text{meas}}$, are then used in the likelihood function (the statistical model for the measurement errors) to compute the weights of the particles. This process is then sequentially repeated for future times to estimate the state variables. Although simple, this algorithm may degenerate the particles, that is, the majority of particles may have negligible weights. The degeneracy phenomenon can be overcome with a resampling step in the particle filter, which eliminates particles with small weights and generates new particles from those with large weights [15–25]. In the SIR algorithm [17, 18] used in this work, the resampling step is applied every time step. Table 1 summarizes the SIR algorithm.

Table 1. Sampling Importance Resampling (SIR) algorithm [17, 18].

Step 1
For $i = 1, ..., N$ draw new particles $\mathbf{y}_k^i$ from the prior density $\pi\left(\mathbf{y}_k \mid \mathbf{y}_{k-1}^i, \boldsymbol{\theta}\right)$ and then use the likelihood density to calculate the corresponding weights $w_k^i = \pi\left(\mathbf{z}_k \mid \mathbf{y}_k^i, \boldsymbol{\theta}\right)$.
Step 2
Calculate the total weight $T_w = \sum_{i=1}^{N} w_k^i$ and then normalize the particle weights, that is, for $i = 1, ..., N$ let $w_k^i = T_w^{-1} w_k^i$.
Step 3
Resample the particles as follows: Construct the cumulative sum of weights (CSW) by computing $c_i = c_{i-1} + w_k^i$ for $i = 1, ..., N$, with $c_0 = 0$. Let $i = 1$ and draw a starting point u_1 from the uniform distribution $U\left[0, N^{-1}\right]$ For $j = 1, ..., N$ Move along the CSW by making $u_j = u_1 + N^{-1}(j-1)$ While $u_j > c_i$ make $i = i + 1$ and Assign sample $\mathbf{y}_k^j = \mathbf{y}_k^i$ Assign sample weight $w_k^j = N^{-1}$.

The measurements are assumed here as uncorrelated and containing additive Gaussian noises, with zero means and a constant covariance matrix $\mathbf{R}$. Therefore, the observation model can be written as

$$\mathbf{z}_k = \mathbf{g}_k(\mathbf{y}_k, \theta) + \mathbf{n}_k, \tag{5}$$

where $\mathbf{n}_k = N(\mathbf{0}, \mathbf{R})$. With such hypotheses about the measurement errors, the likelihood function, which is used for the computation of the weights in the particle filter method, is thus given by:

$$\pi(\mathbf{z}_k \mid \mathbf{y}_k, \boldsymbol{\theta}) = (2\pi)^{-I/2} |\mathbf{R}|^{-1/2} \exp\left\{-\frac{1}{2}\left[\mathbf{z}_k^{\text{meas}} - \mathbf{g}_k(\mathbf{y}_k, \boldsymbol{\theta})\right]^T \mathbf{R}^{-1}\left[\mathbf{z}_k^{\text{meas}} - \mathbf{g}_k(\mathbf{y}_k, \boldsymbol{\theta})\right]\right\}, \tag{6}$$

where I is the number of measurements at each time instant t_k, and $\pi = 4\tan^{-1}(1)$. The vector of model parameters $\boldsymbol{\theta}$ is assumed as known in this work, but the related uncertainties are accounted for in the noise vectors $\mathbf{v}_k$ and $\mathbf{n}_k$.

4. Results and discussions

For the results presented below, the radiuses that limit each tissue layer in the head were considered as $r_1 = 42$ mm, $r_2 = 53$ mm, $r_3 = 55$ mm and $r_4 = 57$ mm [9, 26], while the thickness of the cooling channel was taken as $H = 5$ mm. By following the experimental results presented in [10], the global heat transfer coefficient from the surface of the head to the cooling water was considered as 225 $\mathrm{Wm^{-2}K^{-1}}$ and the water mass flow rate as 0.012 $\mathrm{kg \cdot s^{-1}}$. The water in the cap was assumed initially in thermal equilibrium with the surroundings at the temperature $T_\infty = 18°\mathrm{C}$. During the treatment, the water temperature at the inlet of the cap was maintained at $T_{l,I} = 15°\mathrm{C}$. Since this work is focused on the start of the cooling treatment, the arterial blood temperature was also assumed constant and given by $T_a = 37°\mathrm{C}$. The thermophysical properties used for the different tissues, as well as for blood and water, are summarized in Table 2 [1, 26].

Table 2. Thermophysical properties of the different tissues [1, 26].

	Properties				
	k [W $\mathrm{m^{-1}K^{-1}}$]	ρ [kg $\mathrm{m^{-3}}$]	c [W $\mathrm{kg^{-1}K^{-1}}$]	ω_0 [$\mathrm{s^{-1}}$]	q_0 [W $\mathrm{m^{-3}}$]
Scalp	0.34	1000	4000	3.33×10^{-4}	363.4
Skull	1.16	1500	2300	3×10^{-4}	368.3
Gray matter	0.5	1050	3700	1.33×10^{-2}	16700
White matter	0.5	1050	3700	3.33×10^{-3}	4175
Blood	0.5	1050	3800	–	–
Water	0.6	1000	4180	–	–

The conditions examined in this work included healthy and ischemic brains. Ischemia was supposed to take place either in the total white and gray matter regions or in part of the gray matter, as depicted in Fig. 2.

Based on a grid convergence analysis, the number of finite volumes selected for the discretization of the region of the head (Eqs (1)) was 57 ×57 (r and θ directions, respectively). The region of the cap (Eqs (2)) was then discretized with 57 volumes in the θ direction for compatibility with the mesh for the head region. A time step of 10^{-3} s was used for the stability of the solution, which involved an explicit time integration scheme. With such number of finite volumes and time step, discrepancies were about 1% among the steady-state heat rates that were: (i) generated inside the head, (ii) transferred to the water and (iii) transferred by conduction at the head surface.

The initial temperature in the region of the head was obtained from the steady state solution of the bioheat transfer problem (Eqs (1)) before the cooling treatment was initiated, by considering heat transfer from the head to the surroundings at $T_\infty = 18°\mathrm{C}$, with a heat transfer coefficient of 10 $\mathrm{Wm^{-2}K^{-1}}$. Figures 3a and 3b present the initial conditions for the cases of healthy and partially ischemic brains, respectively.

To solve the state estimation problem, the uncertainties in the evolution model were assumed as additive and Gaussian. The means and standard deviations for such uncertainties were obtained from the Monte Carlo simulations of the direct problem for a healthy brain, by sampling the model parameters from Gaussian distributions centered on the values presented in Table 2, with standard deviations given by 1% of these mean values. The transient variation of the temperature standard deviations, obtained from 500 simulations of the direct problem, is presented in Fig. 4b

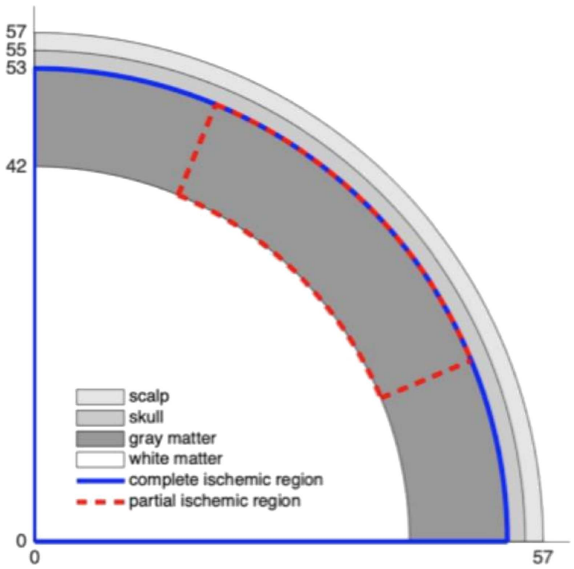

Fig. 2. Healthy and ischemic brain conditions considered in this work.

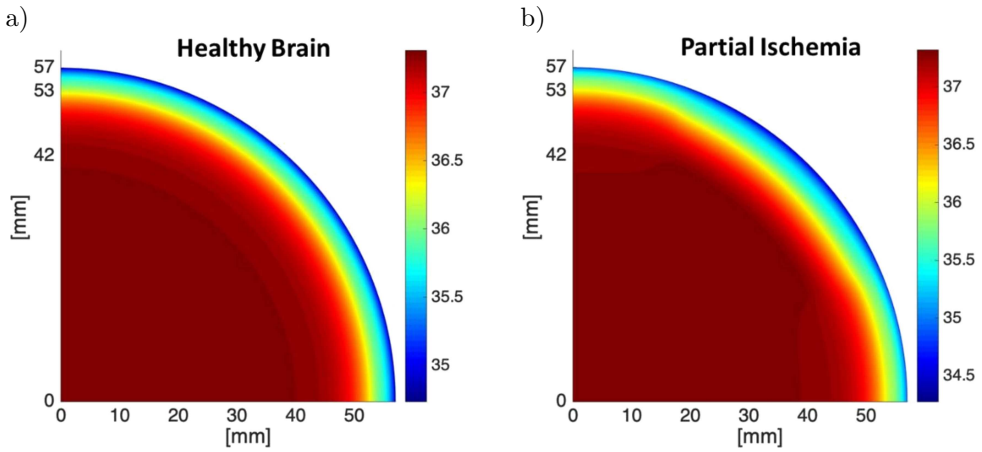

Fig. 3. The initial condition for: a) healthy brain; b) partially ischemic brain.

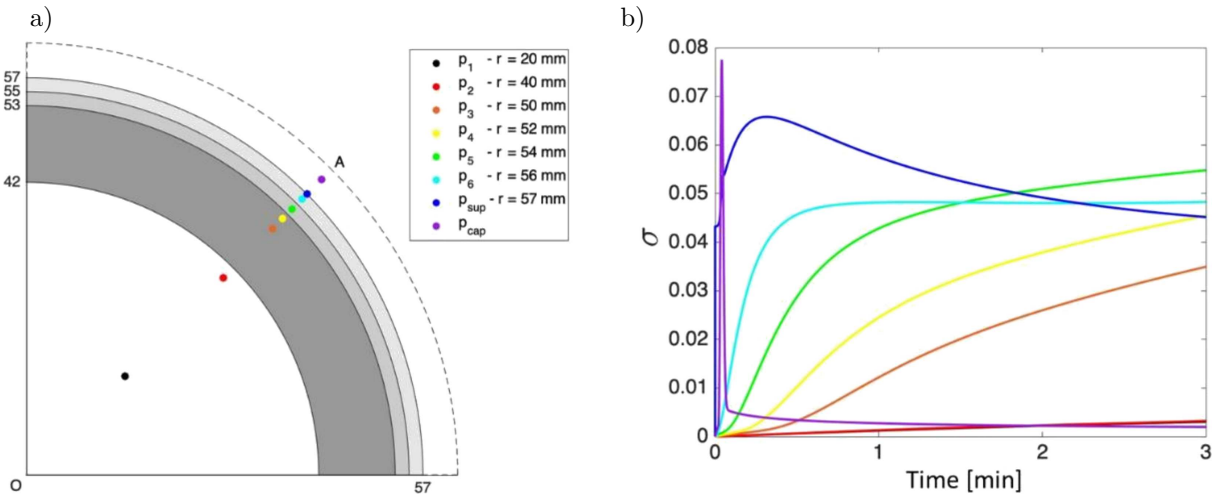

Fig. 4. a) Points used for the analyses; b) temperature standard deviations obtained with the Monte Carlo simulations of the direct problem at the selected points.

for the selected points shown in Fig. 4a. The temperature standard deviations are smaller for the internal regions, far from the head surface where the cooling takes place. Based on the values presented in Fig. 4b, the standard deviations in each tissue layer and water were then considered uniform for the simulations presented below.

The effects of the number of sensors and the number of particles on the inverse problem solution, obtained with the SIR algorithm of the particle filter method, will now be examined. For this analysis, we considered the first 60 seconds of the cooling of a healthy brain, with a measurement frequency of 1000 Hz and a standard deviation of 0.3°C for the simulated measurements. Table 3 presents the RMS errors of the solutions obtained with different numbers of sensors and particles, while Figs 5a and 5b illustrate the configurations with 4 and 10 sensors, respectively. Table 3 shows that the RMS errors are not affected by increasing the number of particles and the number of sensors for the present inverse problem. The RMS error is defined as

$$e_{\mathrm{RMS}} = \frac{1}{MP}\sqrt{\sum_{m=1}^{M}\sum_{p=1}^{P}\left[T^{m}_{p,exa} - T^{m}_{p,est}\right]^2}, \tag{7}$$

where the subscripts *exa* and *est* refer to the exact and estimated temperatures, respectively, at the finite volume p and at the time step m. P and M are the numbers of finite volumes and time steps, respectively.

Table 3. RMS errors.

	500 particles	1000 particles
4 sensors	9×10^{-7}	9×10^{-7}
8 sensors	10×10^{-7}	9×10^{-7}
10 sensors	10×10^{-7}	9×10^{-7}
58 sensors	7×10^{-7}	7×10^{-7}

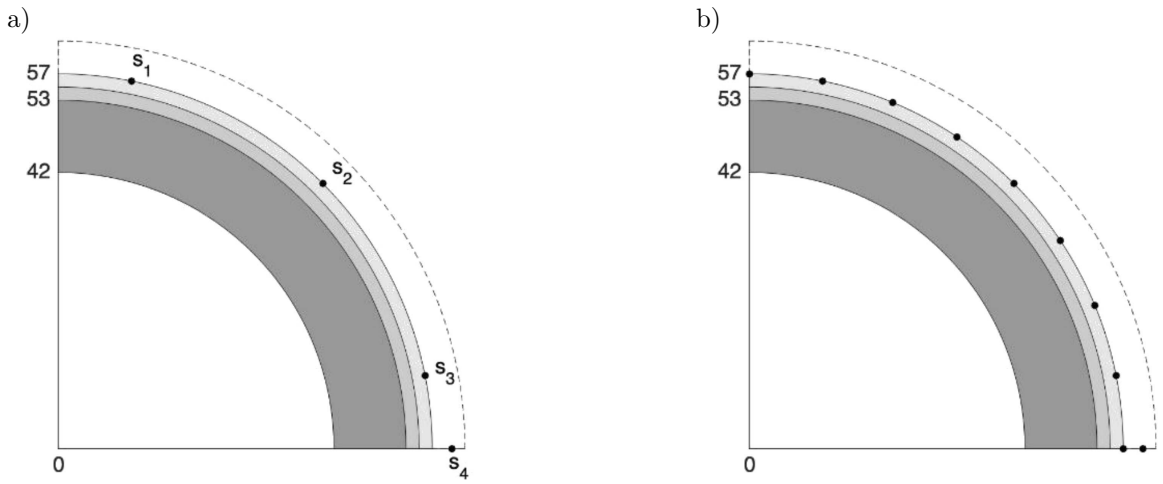

Fig. 5. Configuration with: a) 4 sensors; b) 10 sensors.

We now consider the solution of the state estimation problem for the conditions of healthy and ischemic brains, during the first 5 minutes of the local cooling treatment. Since the RMS errors were not affected by the numbers of particles and sensors, to avoid large computational times we considered the results obtained for 500 particles, and to avoid patient discomfort we used 4 sensors. The simulated measurements were assumed to have a frequency of 2 Hz and contained

Gaussian errors with a standard deviation of 0.3°C [10]. Computational times of each run were around 9 hours, with a MATLAB code running in a computer with processor Intel® CoreTM i7-7700U and 16 GB RAM.

Figure 6a presents a comparison of the estimated and exact temperatures at the sensor location S_2 (see Fig. 5a) for the healthy brain, and it also presents the simulated measurements and the 99% confidence intervals of the estimated temperatures. Figure 6a also shows that the estimated temperatures were in better agreement with the exact temperatures than the measurements. This result is more apparent in Fig. 6b – a close-up of Fig. 6a in the first minute of the treatment. Similar results are presented in Figs 7a and 7b, for the sensor location S_4 (see Fig. 5a) which corresponds to the water temperature at the channel outlet. Furthermore, accurate estimations for the internal brain temperature could be obtained at points where the measurements were not available, as shown in Figs 8a and 8b, for points P_2 and P_3 (see Fig. 4a), respectively. We note that the temperature at point P_2 in the white matter was slightly reduced during the cooling period of 5 minutes. This is also evident from the analysis of Figs 9a and 9b, which present the exact and the estimated means obtained with the particle filter method, respectively, for the healthy brain at time $t = 5$ min. The same figures show accurate estimated whole head temperatures, including the regions far from the measurement points, such as the white matter. The estimated temperatures were smooth, but some blurring and oscillations can be observed in Fig. 9b and this is a result of

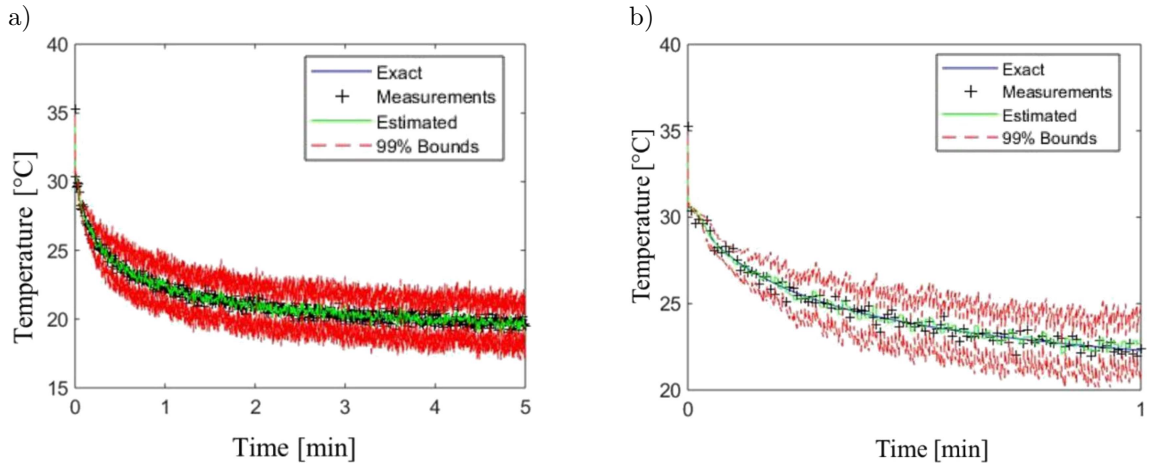

Fig. 6. The solution of the state estimation problem for a healthy brain at the position of sensor S_2: a) time period of 5 minutes; b) close-up Fig. 6a in the first minute.

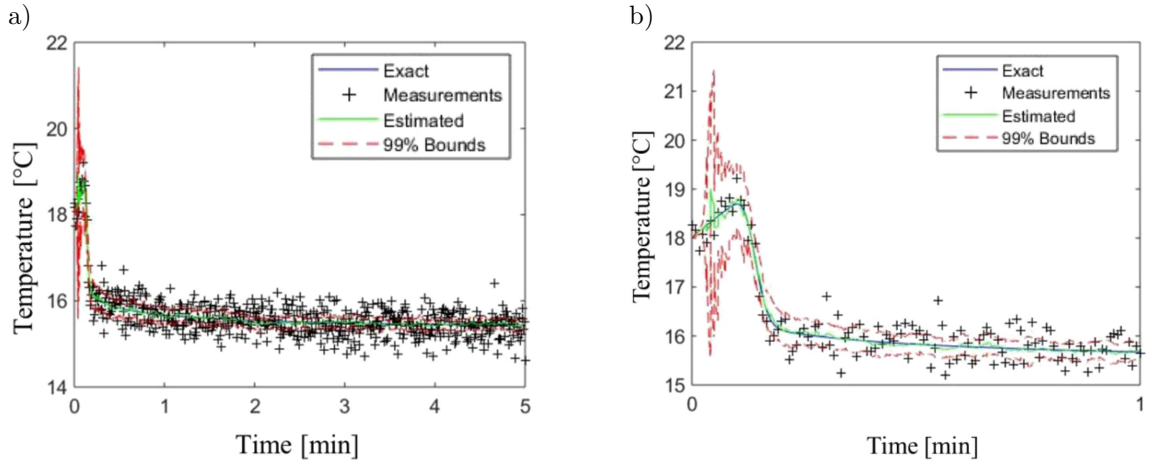

Fig. 7. The solution of the state estimation problem for a healthy brain at the position of sensor S_4: a) time period of 5 minutes; b) close-up of Fig. 7a in the first minute.

the ill-posed character of the inverse problem. The temperature distribution in the cooling water was also quite accurately estimated for the healthy brain, as shown in Figs 10a and 10b.

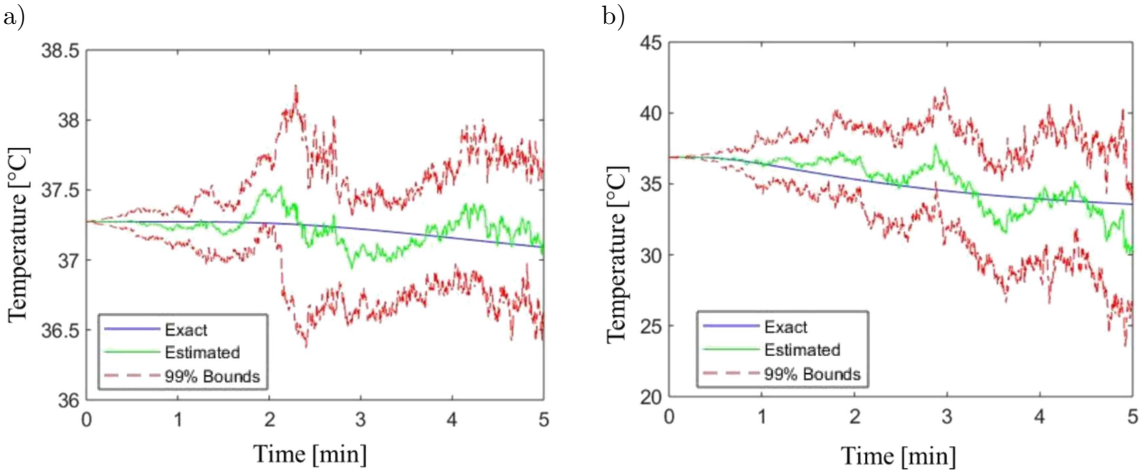

Fig. 8. The solution of the state estimation problem for a healthy brain at: a) P_2; b) P_3.

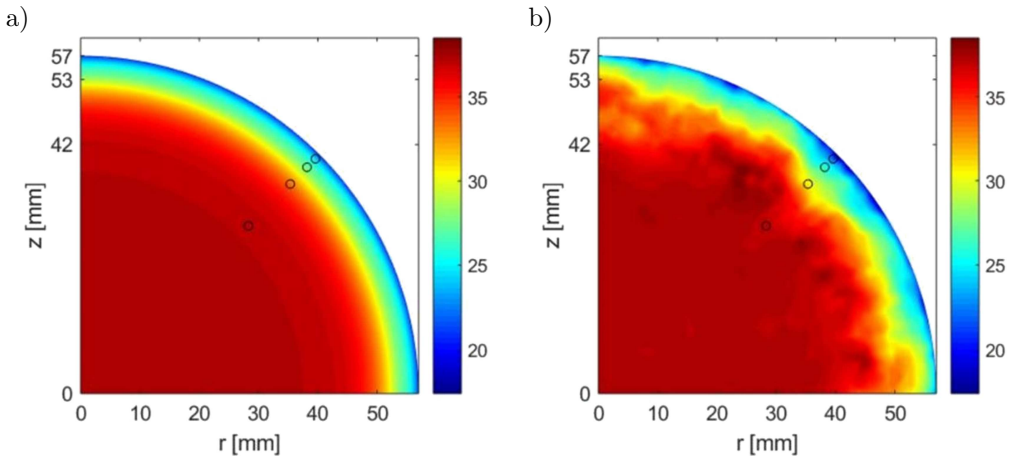

Fig. 9. Temperatures in the healthy brain at $t = 5$ min: a) exact; b) estimated means obtained with the particle filter.

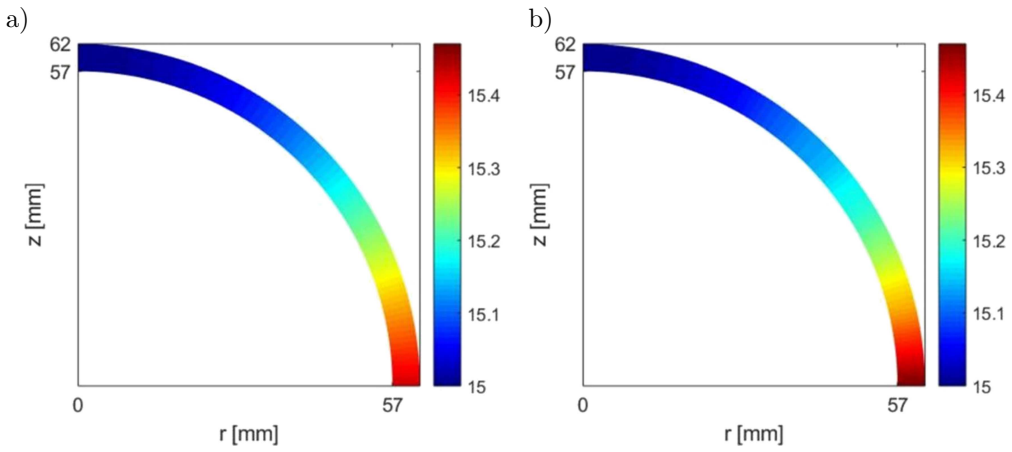

Fig. 10. Temperatures in the cooling water at $t = 5$ min: a) exact; b) estimated means obtained with the particle filter.

It is interesting to note that the particle filter not only provides the estimation of accurate means for the state variables, as observed in Figs 6–10, but also reduces the uncertainties associated with the estimated quantities. Figure 11 is an illustration of this as it presents the results of the a Monte Carlo simulation of the evolution model at the measurement location S_2, without taking into account the information provided by the measurements. Although Fig. 11 shows an excellent agreement between the estimated means of the Monte Carlo simulation and the exact temperatures, the uncertainties associated with such estimation are more significant than those obtained with the solution of the state estimation problem with the particle filter (see Fig. 6a). As expected, the reduction of uncertainties is more significant in the regions near the measurement locations. Regions far from the measurements are less affected by the likelihood function in the particle filter method and rely mostly on the evolution model. This is clear from the comparison of Figs 12a and 12b, which present the estimated standard deviations for the temperatures in the head at $t = 5$ min for a healthy brain, obtained with the particle filter and with the pure Monte Carlo simulations, respectively. Except for a few small regions, the standard deviations estimated by the particle filter are much smaller than those of the Monte Carlo simulations in the scalp, skull and parts of the gray matter. On the other hand, the standard deviations in the white matter result from the application of the evolution model, and similar values were found with the particle filter method and the Monte Carlo simulations.

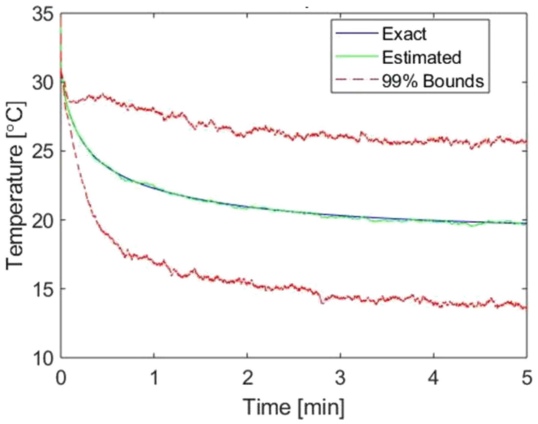

Fig. 11. Monte Carlo simulation for a healthy brain at the position of sensor S_2.

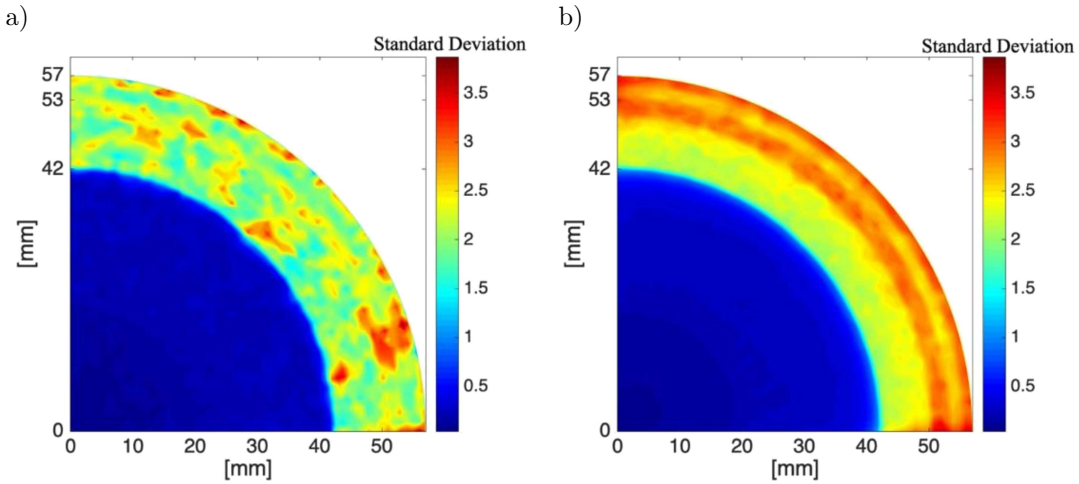

Fig. 12. Standard deviations for temperature in a healthy brain at $t = 5$ min: a) the solution of the state estimation problem; b) the Monte Carlo simulations.

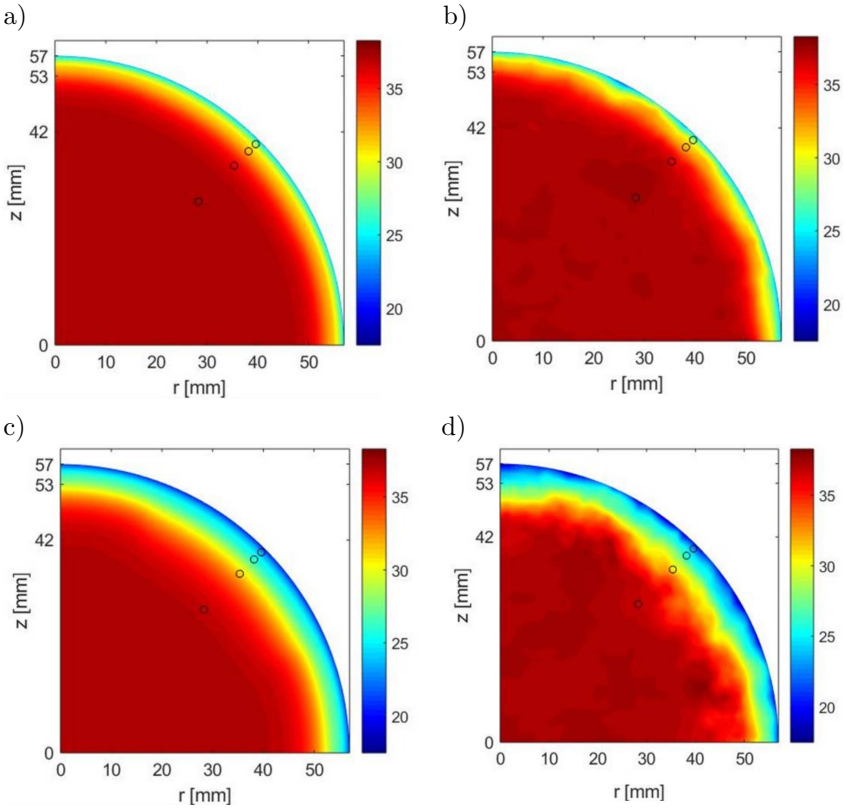

Fig. 13. Temperatures in a partial ischemic brain: a) exact at $t = 1$ min; b) estimated at $t = 1$ min; c) exact at $t = 5$ min; d) estimated at $t = 5$ min.

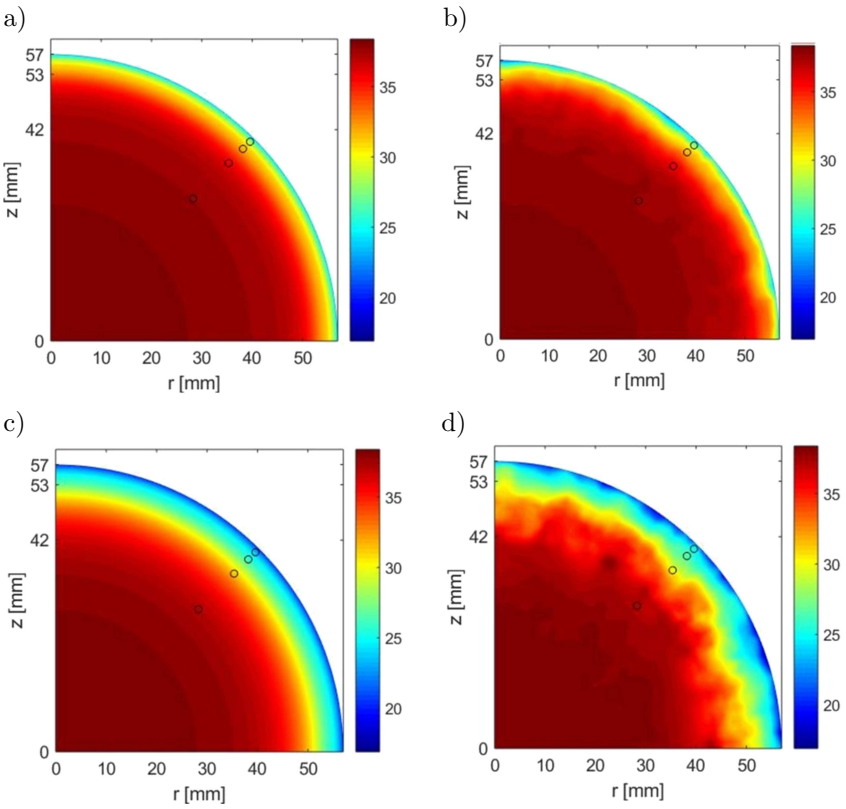

Fig. 14. Temperatures in a full ischemic brain: a) exact at $t = 1$ min; b) estimated at $t = 1$ min; c) exact at $t = 5$ min; d) estimated at $t = 5$ min.

The temperatures estimated with the particle filter method for brains with partial and total ischemia are compared to the corresponding exact values in Figs 13a–13d and 14a–14d, respectively, at times $t = 1$ min and $t = 5$ min. As for the healthy brain, the analysis shown in Figs 13 and 14 also reveals the accurate estimation of the transient temperature distributions for these two ischemic conditions, which were obtained with the solution of a state estimation problem with the SIR algorithm of the particle filter method.

5. Conclusions

In this paper, we solved a state estimation problem with the SIR algorithm of the particle filter method, for the bioheat transfer problem in the head of a newborn, during the local cooling treatment of neonatal hypoxic-ischemic encephalopathy. This work aimed at the sequential estimation of the internal temperature of the head, by using non-invasive temperature measurements taken at the head surface and the outlet of the water channel. Simulated measurements were used in the inverse analysis for a healthy brain, as well as for conditions of total ischemia (in the white and gray matters) and partial ischemia (in a region of the gray matter). The numbers of particles and sensor positions were selected by examining the RMS error of the inverse problem solution.

The state estimation problem was solved with 500 particles, in order to avoid large computational times, and 4 sensors, in order to avoid patient discomfort. The means estimated for the transient temperatures were in excellent agreement with the exact temperatures for the three conditions (healthy brain, partial ischemia and full ischemia) examined here. Moreover, it was also shown that uncertainties in the head temperatures could be drastically reduced with the solution of the state estimation problem. The reduction of uncertainties was more significant in the regions near the measurement locations. On the other hand, regions far from the measurements, such as the white matter, were less affected by the likelihood function in the particle filter method and relied mostly on the evolution model.

The present work can be applied in the future for active control of the local cooling treatment of neonatal hypoxic-ischemic encephalopathy, by acting as a method of monitoring the internal head temperatures. Nevertheless, computational times need to be reduced for practical applications.

Acknowledgments

The support provided by CNPq and FAPERJ, the agencies of the Brazilian and Rio de Janeiro state governments, is gratefully appreciated. This study was financed in part by Coordenação de Aperfeiçoamento de Pessoal de Nível Superior – Brazil (CAPES) – Finance Code 001. The research of AJN was supported by the National Science Centre, Poland within the project number UMO-2018/29/B/ST8/01490.

Author disclosure statement

There are no relationships of the authors with any people or organizations that could inappropriately influence (bias) this work.

References

[1] J.E. Laszczyk, A.J. Nowak. *The Analysis of a Newborn's Brain Cooling Process*. LAP LAMBERT Academic Publishing, 2015.

[2] J.E. Laszczyk, A. Mączko, W. Walas, A.J. Nowak. The numerical modelling of the heat transfer processes within neonate's body based on the simplified geometric model. *Information Technologies in Biomedicine, Lecture Notes in Computer Science*, **7339**: 310–318, 2012.

[3] F.C. Barone, G.Z. Feuerstein, R.E. White. Brain cooling during transient focal ischemia provides complete neuroprotection. *Neuroscience and Biobehavioral Reviews*, **21**(1): 31–44, 1997.
[4] R.S.B. Clark, P.M. Kochanek, D.W. Marion, J.K. Schiding, M. White, A.M. Palmer, S.T. DeKosky. Mild post traumatic hypothermia reduces mortality after severe controlled cortical impact in rats. *Journal of Cerebral Blood Flow and Metabolism*, **16**(2): 253–261, 1996.
[5] D.W. Marion, L.E. Penrod, S.F. Kelsey, W.D. Obrist, P.M. Kochanek, A.M. Palmer, S.R. Wisniewski, S.T. DeKosky. Treatment of traumatic brain injury with moderate hypothermia. *The New England Journal of Medicine*, **336**: 540–546, 1997.
[6] P.D. Gluckman, J.S. Wyatt, D. Azzopardi, R. Ballard, A.D. Edwards, D.M. Ferriero, R.A. Polin, Ch.M. Robertson, M. Thoresen, A. Whitelaw, A.J. Gunn. Selective head cooling with mild systemic hypothermia after neonatal encephalopathy: multicentre randomised trial. *The Lancet*, **365**(9460): 663–670, 2005.
[7] G. Kuhnen, N. Einer-Jensen, S.A. Tisherman. Cooling methods. In: S.A. Tisherman, F. Sterz [Eds], *Therapeutic Pypothermi*, pp. 211–233. Springer, Boston, 2005.
[8] S.A. Zanelli, D.P. Stanley, D.A. Kaufman. Hypoxic-Ischemic Encephalopathy. *Medscape*, 2008.
[9] C. Diao, L. Zhu, H. Wang. Cooling and rewarming for brain ischemia or injury: theoretical analysis. *Annals of Biomedical Engineering*, **31**(3): 346–353, 2003.
[10] D. Bandoła, A.J. Nowak, M. Rojczyk, Z. Ostrowski, W. Walas. Measurement and computational experiments within newborn's brain cooling process. In: *International Heat Transfer Conference Digital Library*, pp. 551–558. Begell House Inc., 2018, DOI: 10.1615/IHTC16.bma.022900.
[11] B.H. Dennis, R.C. Eberhart, G.S. Dulikravich, S.W. Radons. Finite-element simulation of cooling of realistic 3-D human head and neck. *Journal of Biomechanical Engineering*, **125**(6): 832–840, 2003.
[12] C. Pacheco, H.R.B. Orlande, M.J. Colaço, G.S. Dulikravich. State estimation problems in PRF-shift magnetic resonance thermometry. *International Journal of Numerical Methods for Heat & Fluid Flow*, **28**(2): 315–335, 2018.
[13] M. Alaeian, H.R.B. Orlande, B. Lamien. Application of the photoacoustic technique for temperature measurements during hyperthermia. *Inverse Problems in Science and Engineering*, **10**: 1–21, 2018.
[14] M. Alaeian, H.R.B. Orlande. Inverse photoacoustic technique for parameter and temperature estimation in tissues. *Heat Transfer Engineering*, **38**(18): 1573–1594, 2016.
[15] A. Doucet, N. de Freitas, N. Gordon. *Sequential Monte Carlo Methods in Practice*. Springer, New York, 2001.
[16] J. Kaipio, E. Somersalo. *Statistical and Computational Inverse Problems, Applied Mathematical Sciences*. Springer-Verlag, New York, 2004.
[17] B. Ristic, S. Arulampalam, N. Gordon. *Beyond the Kalman Filter*. Artech House, Boston, 2004.
[18] S. Arulampalam, S. Maskell, N. Gordon, T. Clapp. A tutorial on particle filters for on-line non-linear/non-Gaussian Bayesian tracking. *IEEE Transactions on Signal Processing*, **50**: 174–188, 2001.
[19] C. Andrieu, C.P. Robert, A. Doucet. Computational advances for and from Bayesian analysis. *Statistical Science*, **19**(1): 118–127, 2004.
[20] C. Andrieu, A. Doucet, S.S. Singh, V.B. Tadic. Particle methods for change detection, system identification and control. *Proceedings of the IEEE*, **92**(3): 423–438, 2004.
[21] J. Carpenter, P. Clifford, P. Fearnhead. Improved particle filter for non-linear problems. *IEE Proceedings – Radar, Sonar and Navigation*, **146**(1): 2–7, 1999.
[22] N. Kantas, A. Doucet, S.S. Singh, J. Maciejowski, N. Chopin. On particle methods for parameter estimation in state-space models. *Statistical Science*, **30**(3): 328–351, 2015.
[23] P. Del Moral, A. Doucet, A. Jasra. Sequential Monte Carlo samplers. *Journal of the Royal Statistical Society: Series B (Statistical Methodology)*, **68**(3): 411–436, 2006.
[24] H.F. Lopes, C.M. Carvalho. Online Bayesian; learning in dynamic models: an illustrative introduction to particle methods. In: P. Damien, P. Dellaportas, N.G. Polson, D.A. Stephens. *Bayesian Theory and Applications*, Chapter 11, Oxford University, 2013.
[25] H.R.B. Orlande, M.J. Colaço, G.S. Dulikravich, F. Vianna, W. da Silva, H.M. Fonseca. O. Fudym. State estimation problems in heat transfer. *International Journal for Uncertainty Quantification*, **2**: 239–258, 2012.
[26] L. Zhu, C. Diao. Theoretical simulation of temperature distribution in the brain during mild hypothermia treatment for brain injury. *Medical & Biological & Engineering & Computing*, **39**: 681–687, 2001.
[27] H.H. Pennes. Analysis of tissue and arterial blood temperatures in the resting human forearm. *Journal of Applied Physiology*, **1**(2): 93–122, 1948.
[28] X. Xu, P. Tikuisis, G. Giesbrecht. A mathematical model for human brain cooling during cold-water near-drowning. *Journal of Applied Physiology*, **86**(1): 265–272, 1999.